

# NUMERICAL SIMULATIONS OF OSCILLATORY FLOW OVER SAND RIPPLES

Thomas Pierro<sup>1</sup>, Donald Slinn<sup>1</sup>, Kraig Winters<sup>2</sup>

<sup>1</sup> Department of Ocean Engineering, Florida Atlantic University, Boca Raton, Florida • <sup>2</sup> Applied Physics Laboratory, University of Washington, Seattle, Washington

Supported by the US Office of Naval Research • AGU Fall Meeting 2000 • Poster OS72A-09

## BACKGROUND

The wave bottom boundary layer refers to the thin layer of fluid that lies closest to the seabed that can dissipate significant energy from shoaling surface waves in a turbulent shear flow near the ocean floor.

### Wave Bottom Boundary Layer (WBBL)

- Complex nonlinear relationships in a thin layer of high vorticity.
- Oscillatory fluid motion caused by surface gravity waves interacts with the seabed.
- Turbulent dissipation caused by shear instabilities and flow separation over a rough boundary is a sink for wave energy.
- Sand particles become entrained in the water column and are redistributed to form sand ripples.
- Ripples influence the flow by increasing wall roughness and dissipation rates.

This work is part of the ONR Shoaling Waves Initiative, complimenting field measurements of the bottom boundary layer conducted by T. Stanton and E. Thornton of the Naval Postgraduate School during the fall of 1999 at the Field Research Facility in Duck, N.C.

## MOTIVATING QUESTIONS

- How is the fluid dynamics in the WBBL influenced by the topography of the seabed?
- What forces does the oscillatory flow caused by surface waves produce on the ripples?
- Under what conditions does the WBBL become turbulent?
- How do wave energy dissipation rates depend on ripple shape, length, and amplitude?
- How does the presence of rippled topography affect the incident wave field?

## MODEL FORMULATION

Our computational fluid dynamic (CFD) model is a mathematical model that solves the three-dimensional, unsteady, Navier-Stokes equation for an incompressible, homogeneous fluid on curvilinear coordinates. With this model, we simulate turbulent boundary layer flows over rippled topographies in a small periodic domain of the order of  $100 \text{ cm}^3$ .

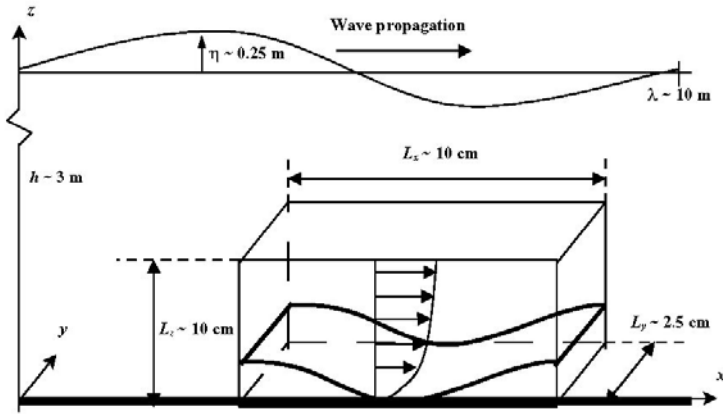


**Figure 1.** Sketch of the problem geometry.

The characteristic Reynolds numbers of the flow ( $Re = U_m \delta_t / \nu$ ) are based on the turbulent boundary layer thickness  $\delta_t$  and are of the order of 20,000.

Although the model has the ability to perform Large Eddy Simulations (LES), the results presented here are from Direct Numerical Simulations (DNS) to better represent the small scales associated with boundary layer flow. Other model features include:

- Third-order Adams-Bashforth variable time step
- Fourth-order compact spatial differencing
- A Poisson equation pressure solver using a fourth-order multi-grid method (MudPack)
- Capability to simulate complex bottom topographies

The flow is forced with a horizontal pressure gradient simulating a passing surface gravity wave, which induces an oscillatory free stream velocity external to the boundary layer of the form:

$$U = U_m \sin(\omega t)$$

Where,  $U_m$  is the maximum wave-induced near bed velocity and  $\omega = 2\pi/T$  is the wave frequency.

The bottom boundary is a fixed rigid wall (sand ripple) satisfying the “no-slip” boundary condition, while the top boundary is a fixed rigid lid allowing “free-slip” conditions.

The four horizontal boundaries of the domain are periodic in order to simulate the flow conditions over an infinite number of ripples.

We use  $129 \times 33 \times 129$  ( $n_x \times n_y \times n_z$ ) grid points for a domain size of  $[L_x, L_y, L_z] = [10, 2.5, 10]$  cm, to ensure a grid spacing near the boundary of the order of 0.1 mm normal to the wall and 0.5 mm along the wall.

## GRID TRANSFORMATION

Due to the complex nature of the terrain, the geometry is mapped to curvilinear coordinates matching the topography and the equations are solved with a grid transformation matrix for contravariant variables ( $U, v, W, P$ ). The solutions are then mapped back to the Cartesian grid for interpretation as physical variables ( $u, v, w, p$ ).

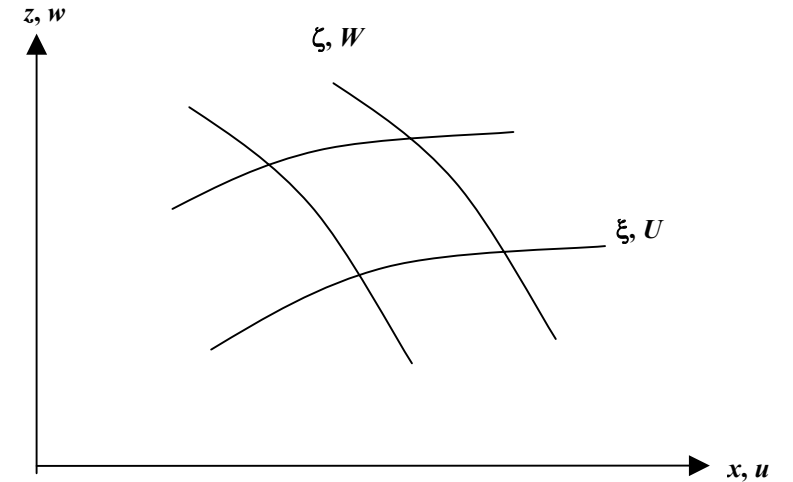


**Figure 2.** Coordinate systems ( $x$ - $z$ ) and ( $\xi$ - $\zeta$ ) for the model.

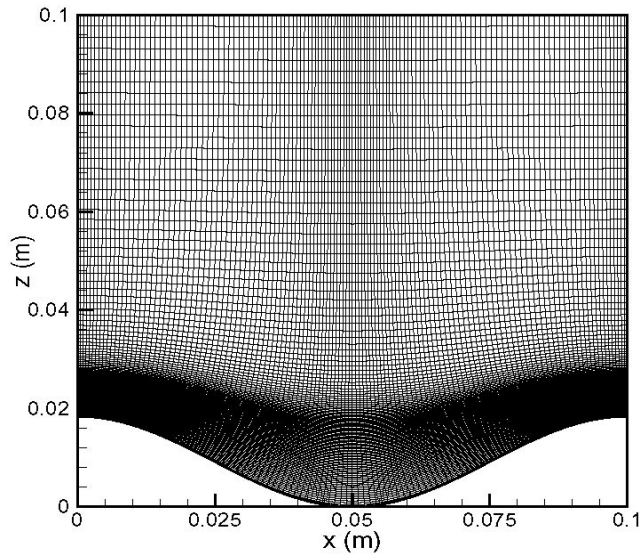


**Figure 3.** Grid layout in  $x$ - $z$  plane for a sinusoidal ripple 1.8cm high and 10 cm long.

### GOVERNING EQUATIONS

The Navier-Stokes equations are transformed between the physical variables on a Cartesian grid  $(u, v, w, p)$  and the contravariant variables on a curvilinear grid  $(U, v, W, P)$  with the relations:

$$\begin{bmatrix} u \\ w \end{bmatrix} = \begin{bmatrix} x_\xi & x_\zeta \\ z_\xi & z_\zeta \end{bmatrix} \begin{bmatrix} U \\ W \end{bmatrix} \quad \begin{bmatrix} U \\ W \end{bmatrix} = \frac{1}{|J|} \begin{bmatrix} z_\zeta & -x_\zeta \\ -z_\xi & x_\xi \end{bmatrix} \begin{bmatrix} u \\ w \end{bmatrix}$$

where  $|J| = (x_\xi z_\zeta - x_\zeta z_\xi)$  is the Jacobian determinant of the transformation. From here, the derivatives are formed as,

$$\frac{\partial u}{\partial \xi} = \frac{\partial u}{\partial x} \frac{\partial x}{\partial \xi} + \frac{\partial u}{\partial z} \frac{\partial z}{\partial \xi} \quad \frac{\partial u}{\partial \zeta} = \frac{\partial u}{\partial x} \frac{\partial x}{\partial \zeta} + \frac{\partial u}{\partial z} \frac{\partial z}{\partial \zeta}$$

Now, the momentum equation in the  $x$ -direction for the three-dimensional, incompressible flow:

$$\frac{\partial u}{\partial t} + u \frac{\partial u}{\partial x} + v \frac{\partial u}{\partial y} + w \frac{\partial u}{\partial z} = -\frac{1}{\rho} \frac{\partial p}{\partial x} + \nu \left( \frac{\partial^2 u}{\partial x^2} + \frac{\partial^2 u}{\partial y^2} + \frac{\partial^2 u}{\partial z^2} \right) + F^{(x)}$$

Becomes,

$$\begin{aligned} & \frac{\partial U}{\partial t} + U \frac{\partial U}{\partial \xi} + v \frac{\partial U}{\partial y} + W \frac{\partial U}{\partial \zeta} + \frac{1}{|J|} (z_\zeta x_{\xi\xi} - x_\zeta z_{\xi\xi}) U^2 \\ & + \frac{2}{|J|} (x_{\xi\zeta} z_\zeta - z_{\xi\zeta} x_\zeta) UW + \frac{1}{|J|} (z_\zeta x_{\zeta\zeta} - x_\zeta z_{\zeta\zeta}) W^2 \\ & = -\frac{1}{\rho} \frac{(x_\zeta^2 + z_\zeta^2)}{|J|^2} \frac{\partial P}{\partial \xi} + F^{(\xi)} \\ & + \nu \left\{ z_\zeta \left[ \frac{1}{|J|} (u_{x\xi} z_\zeta - u_{x\zeta} z_\xi + u_{z\xi} x_\xi - u_{z\zeta} x_\zeta) + u_{yy} \right] \right. \\ & \left. - z_\xi \left[ \frac{1}{|J|} (w_{x\xi} z_\zeta - w_{x\zeta} z_\xi + w_{z\xi} x_\xi - w_{z\zeta} x_\zeta) + w_{yy} \right] \right\} \end{aligned}$$

Similarly, the momentum equations for the  $v$  and  $w$  velocities are obtained and the flow is forced with a horizontal pressure gradient,

$$F^{(x)} = U_m \omega \cos(\omega t)$$

## EXPERIMENTS

In 1993, Ranasoma and Sleath studied combined oscillatory and steady flow conditions over sand ripples using laboratory experiments. Utilizing the known wave parameters used to form these ripples, we were able to simulate physically realizable boundary layer flows for different topographies. A passing surface gravity wave, with characteristics:

$$H = 0.54 \text{ m} \quad \bullet \quad L = 9.0 \text{ m} \quad \bullet \quad T = 2.45 \text{ s}$$

will induce maximum particle velocities near the bed of approximately 20 cm/s in 2.8 m of water. Ranasoma and Sleath showed that boundary layer flows of this nature create regular two-dimensional ripples 1.84 cm in height and 10 cm in length. From here, we developed four experimental test cases to determine energy losses associated with the wave conditions:

- **CASE 1:** *Oscillatory flow over a flat bottom*
  - Flat bottom
  - 20 cm/s maximum particle velocity
- **CASE 2:** *Oscillatory flow over sinusoidal ripples*
  - 1.84 cm sine wave ripple
  - 20 cm/s maximum particle velocity
- **CASE 3:** *Oscillatory flow over steep ripples*
  - 1.84 cm steep ripple
  - 20 cm/s maximum particle velocity
- **CASE 4:** *Non-oscillatory flow over steep ripples*
  - 1.84 cm steep ripple
  - 20 cm/s uniform current

## RESULTS

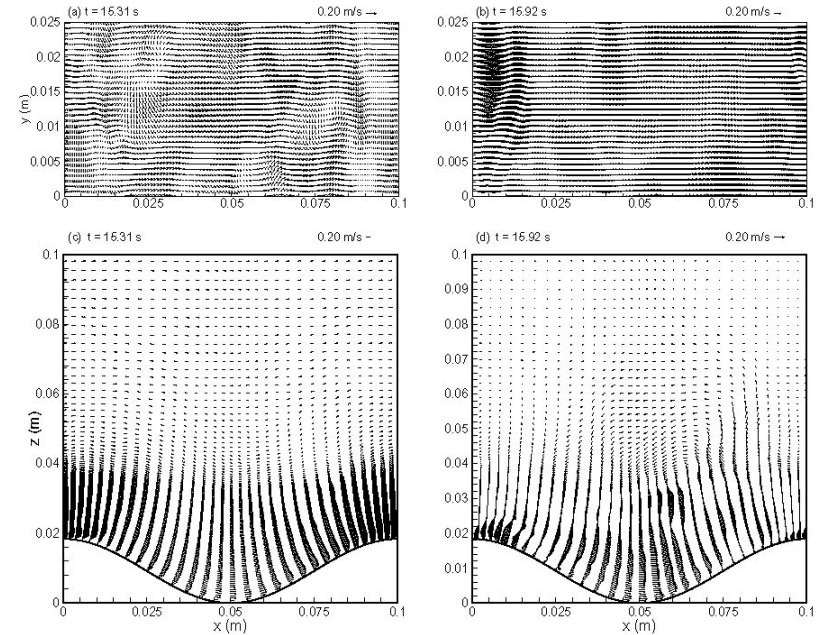


**Figure 4.** Plan views ( $\sigma$ -surface) and cross-sections of velocity vectors for oscillatory flow over a sinusoidal ripple at phases of maximum onshore flow ( $t = 15.31 \text{ s}$ ) and flow reversal ( $t = 15.92 \text{ s}$ ).

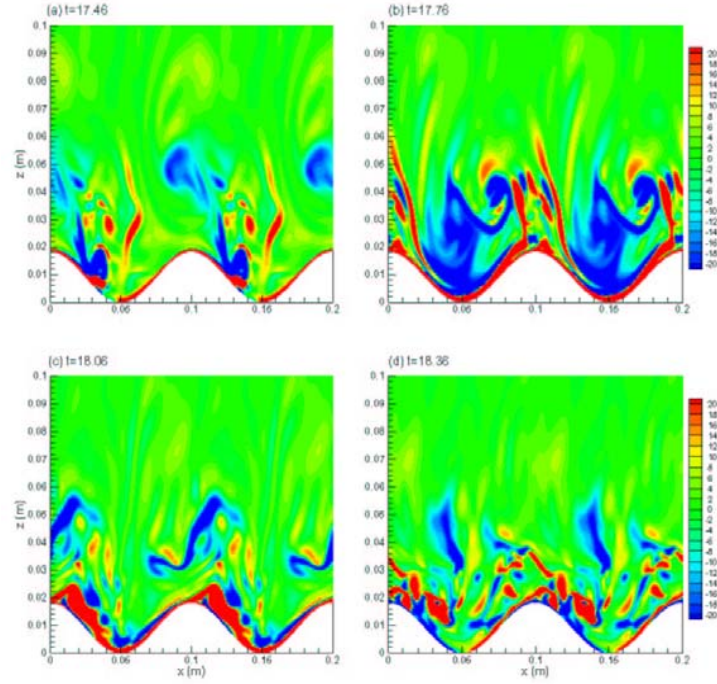


**Figure 5.** Slices of the horizontal vorticity component  $\omega_y \left( s^{-1} \right)$ , in an  $x$ - $z$  plane at  $L_y/2$  for a sinusoidal ripple during phases of (a) flow acceleration, (b) maximum onshore flow, (c) flow deceleration, and (d) flow reversal.

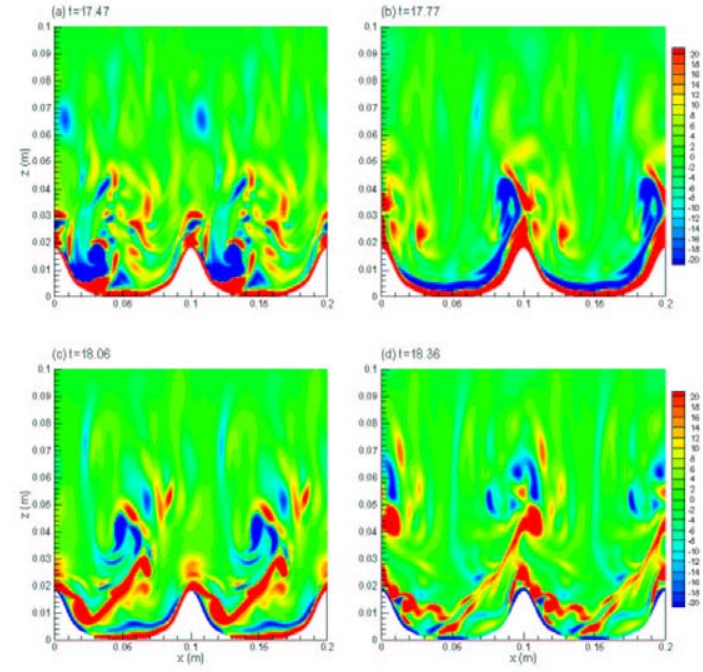


**Figure 6.** Slices of the horizontal vorticity component  $\omega_y \left( s^{-1} \right)$ , in an  $x$ - $z$  plane at  $L_y/2$  for a steep ripple during phases of (a) flow acceleration, (b) maximum onshore flow, (c) flow deceleration, and (d) flow reversal.

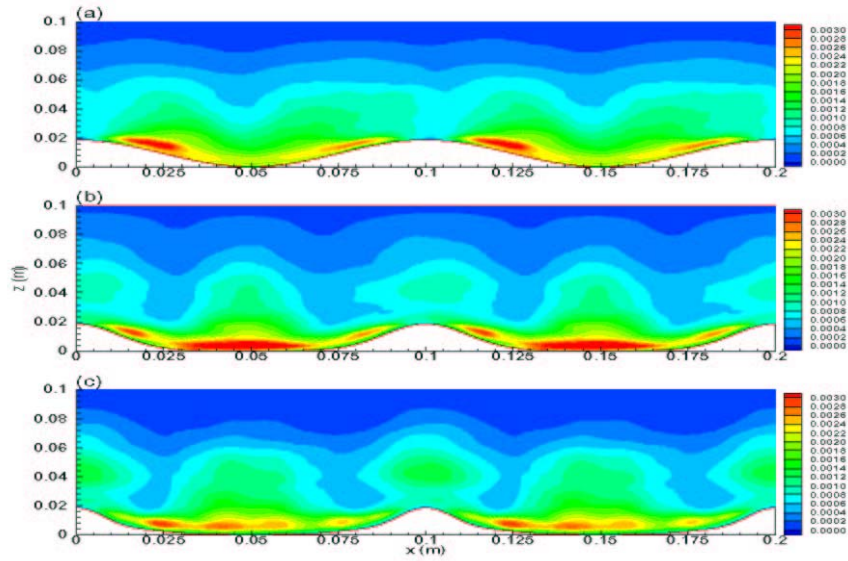


**Figure 7.** Turbulent kinetic energy ( $\text{m}^2 / \text{s}^2$ ) averaged both horizontally ( $y$ -direction) and in time for oscillatory flow over (a) sine, (b) gaussian, and (c) steep ripples.

## RESULTS

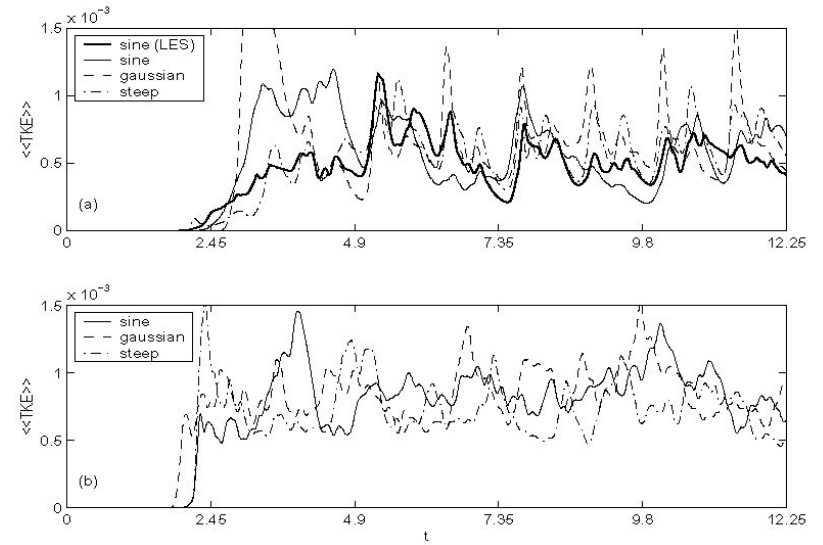


**Figure 8.** Volume averaged turbulent kinetic energy  $\ll TKE \gg$  ( $\text{m}^2 / \text{s}^2$ ) for (a) oscillatory flows and (b) steady flows.

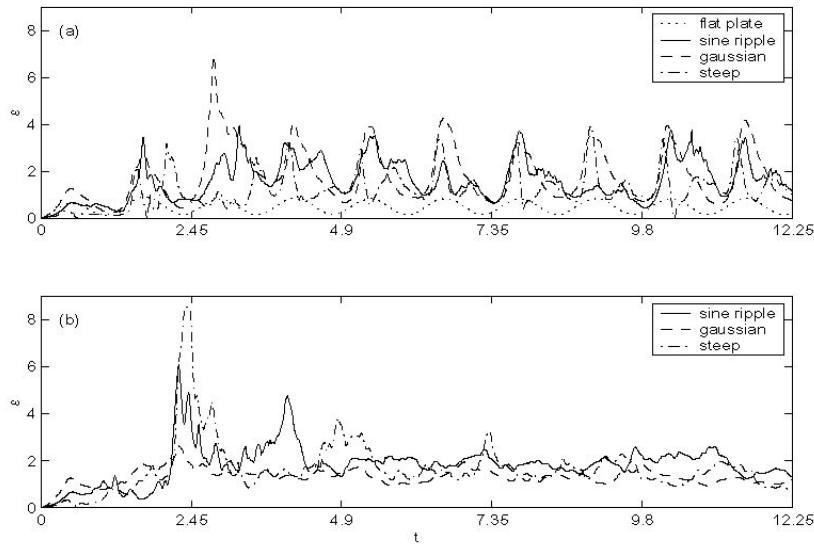


**Figure 9.** Volume averaged dissipation rates ( $W / m^3$ ) for (a) oscillatory and (b) steady cases.

### Dissipation Rates

From these results, we determine the average energy dissipation rates in the boundary layer for each of the oscillatory flow cases:

Case 1:  $0.15 \text{ W/m}^3$

Case 2:  $1.00 \text{ W/m}^3$

Case 3:  $5.00 \text{ W/m}^3$

### Wave Energy

Next, we determine the effect on the passing wave field. The average mechanical energy (per area) of our surface gravity ( $H = 0.54 \text{ m}$ ) wave is calculated:

$$\bar{E} = \frac{1}{8} \rho g H^2 \cong 368 \frac{J}{m^2}$$

### Energy Dissipated

Consider a hypothetical wave propagating in constant depth water  $h = 2.8 \text{ m}$ , with wavelength  $L = 9 \text{ m}$ , period  $T = 2.45 \text{ s}$ , and phase velocity  $3.7 \text{ m/s}$  across a rippled bottom for a distance of  $2 \text{ km}$  taking  $540 \text{ seconds}$ . We estimate the net wave energy dissipated across the boundary layer:

Case 1:  $8 \text{ J/m}^2$

Case 2:  $55 \text{ J/m}^2$

Case 3:  $273 \text{ J/m}^2$

### Percent Decrease in Wave Height

By tracking a single crest in the wave field (in water of constant depth), using the linear approximation, we notice a significant decrease in wave heights over ripples as opposed to a flat bottom. The percent decrease in wave height ( $H_i = 0.54 \text{ m}$ ) for each case:

Case 1 (flat bottom):	1.11 %	$H_f = 0.534 \text{ m}$
Case 2 (sinusoidal ripples):	7.78 %	$H_f = 0.498 \text{ m}$
Case 3 (steep ripples):	49.1 %	$H_f = 0.275 \text{ m}$

## CONCLUSIONS

**In contrast to flows over a flat bottom boundary, the presence of sand ripples has been observed to induce significantly higher turbulence and dissipation rates in the WBBL throughout the full wave period.**

- With the introduction of ripples, boundary layer flows become more complex and highly unsteady, even from the simplest wave field.
- Separation at the ripple crests has been observed to be a mechanism for the production of turbulence in the boundary layer during phases of maximum flow.
- For rippled topographies, turbulent bursts originating during flow reversal are not damped out during flow acceleration (as they are over flat beds) and remain strong throughout the wave period.
- As the steepness of the ripples increase, the turbulence levels rise and relatively large vortex pairs are observed above the rippled crests. This was noted for oscillatory and non-oscillatory flows over steep ripples, but not for flat bottoms or sinusoidal topographies.
- Compared with flat beds, the turbulent kinetic energy and dissipation rates are increased by more than a factor of 6 for sinusoidal ripples and more than a factor of 30 for steep ripples.
- Non-oscillatory flow over steep ripples has been shown to exhibit some similar characteristics in the boundary layer as oscillatory flow over the same topography.
- Over a range of about 2 km of steep ripples, the incident wave height can be shown to decrease (in constant water depth) almost 50% due to energy dissipation in the boundary layer.

## FUTURE WORK

**This project represents only a small portion of the numerical investigations essential to nearshore research. Utilizing computational fluid dynamics, we plan to develop models to gain a new perspective on the fluid processes in the wave bottom boundary layer.**

- Flow over ripples of various shapes and sizes.
- Comparisons of oscillatory and non-oscillatory flows over ripples from varying wave fields.
- Introduction of combined flows, tides, and density stratification.
- Fluid-particle interactions such as sand suspension and redistribution.
- Forcing with time series data from observed wave fields and random wave fields (surface chop).
- Evaluation of 1-D WBBL models such as Grant and Madsen, which performed well for flat bed topographies.